IL NUOVO CIMENTO Vol. 35 C, N. 5 Settembre-Ottobre 2012
DOI 10.1393/ncc/i2012-11316-4

Communications: SIF Congress 2011

Modelling wildfires in the Mediterranean area during summer 2007

C. Pizzigalli on behalf of the Bolchem Group(*)
ISAC-CNR, Sezione di Lecce - Lecce, Italy

ricevuto l' 8 Gennaio 2012; approvato il 14 Marzo 2012

Summary. — The Mediterranean Area is often affected by fires which burn thousands of hectares of vegetation. The biomass burning produces gases and particulates, that spread across thousands of kilometres in the atmosphere, affecting the air quality at the local, regional and global scale. The inclusion of gas and particulate emissions from wildfires in chemistry-transport models is a challenging task because of the large uncertainties related to the detection of fires, the emission factors associated with the type of vegetation and fire characteristics and the injection height of the smoke. This work shows a case study for the summer 2007, a period with fires in Greece, Albania and Algeria. The emission fluxes have been estimated considering the gas species CO, NO_x, SO_2 and NH_3 and the particulate matter $PM_{2.5}$ and PM_{10}. Emission heights for different emitted species have been estimated. The numerical simulations have been performed with the air quality model BOLCHEM. The model results show the effect of fires on air pollution. Moreover, the concentrations of black carbon aerosol predicted by the model are compared with lidar measurements at the Tito Scalo, Potenza (40.63°N, 15.80°E, 760 m a.s.l.), where an unusual layer of aerosol, transported from North Africa, was detected by the PEARL station lidar on 30 August 2007.

PACS 92.60.Sz – Air quality and air pollution.

1. – Introduction

Southern Europe and the Mediterranean basin are frequently affected by fires which can burn thousands of hectares in a few days, especially during summer. In the troposphere, among the major sources of atmospheric pollutants and climate altering species, an important role is played by biomass burning (BB) events (*e.g.* [1]). Previous studies have shown that the atmospheric compounds directly emitted by BB or produced by photochemical processes occurring within BB plumes can be transported over long

(*) Members of the BOLCHEM group that contributed to the present article: R. Cesari, M. D'Isidoro, A. Maurizi and M. Mircea.

distances, from local to regional and global scales, thus affecting both air quality and climate (*e.g.*, [2]). The estimation of emissions from wildfires (species emitted and injection height) is still affected by large uncertainities related to the characteristics of vegetation and of fires. Seiler and Crutzen [3] made first global estimates of fire emissions, which subsequently have been refined and updated (*e.g.*, [1,4,5]). More recently, global satellite-derived burned area information has become available [6, 7]. These datasets have been used in combination with biogeochemical or dedicated fuel load models to estimate emissions [8, 10]. Many available estimation methods and emission predictions are made at global scale (*e.g.*, [9, 10]). These inventories include fires on all global land areas at horizontal resolutions of 1 km to 11 km and typically use a monthly temporal resolution. The lack of inventories with appropriate temporal resolution, at least daily, and horizontal spatial resolutions of order of kilometers, had not allowed realistic fire emission estimates in air quality simulations at regional level. Last year, the Fire INventory from NCAR version 1.0 (FINNv1) has been made available for air quality simulations, providing daily, 1 km resolution, global estimates of the trace gas and particle emissions from open burning of biomass spanning the period 2005–2010 [11, 12]. In comparison to anthropogenic emissions, large forest fires can generate smoke plumes with very large vertical extent due to the release of heat in the combustion process. Determining the correct injection height of emissions is essential since transport and deposition processes are very sensitive to altitude. To account for the buoyancy associated with fires in the chemistry-transport models, fire emissions are commonly distributed within the PBL or in a few layers close to the surface rather than simply at the surface (*e.g.* [13]). Although the low altitude injections can be applied to most fire events, it has been shown [14] that for large fires the emissions need to be injected into the upper troposphere where they can be transported over long distances. Several methods have been proposed in literature to estimate the injection height of emissions. Colarco *et al.* [15] analyzing smoke and pollutants from Canadian forest fires estimate the injection height using remotely sensed and *in situ* data in combination with back trajectory calculations and simulations; Hodzic *et al.* [16] estimate the injection height basing on fire characteristics (such as the fire size or temperature) and atmospheric conditions. In their study on wildfires in Europe during summer 2003, they used a simplified approach adapted from the WRAP method [17] in which the bottom (H_{bot}) and top (H_{top}) altitudes of the fire plume are calculated as a function of the fire buoyant efficiency (BE).

This work introduces a model for estimating the wildfire emissions and injection heights. Both emissions and injection height have been calculated starting from latitude and longitude of wildfires. The emissions have been estimated taking into account the characteristics of soil (vegetation), the area burned and the diurnal cycles of fires. The injection height has been estimated following the WRAP method. The WRAP method has been also used to calculate a diurnal cycle of quantity emitted of gas and particulate. The new fire emissions have been compared with those from the Fire INventory version 1.0 (FINNv1) for the wildfires occurred during the late august 2007 in Greece, Albania and Algeria. Simulations with the air quality model BOLCHEM have been performed and the simulated aerosol concentrations were compared with those detected by lidar at the Tito Scalo, Potenza (40.63° N, 15.80° E, 760 m a.s.l.).

2. – Fire emissions assessment

In order to simulate the dispersion of fire smoke, we calculated the emission fluxes from wildfire and emission height, and we included these emissions in the BOLCHEM model.

2˙1. *Fire emissions fluxes.* – The emission of a species X resulting from fires, $E(X)$, is expressed following the methodology proposed by Seiler and Crutzen [3]:

$$E(X) = A \cdot B \cdot BE \cdot e(X), \tag{1}$$

where A is the burnt area (m^2), B is the fuel load (kg/m^2), BE the burning efficiency and $e(X)$ the emission factor of species X. The fuel load (B) provides the available biomass per surface unit; the burning efficiency (BE) corresponds to the percentage of the biomass which effectively burns. The emission factor gives the amount of chemical species emitted for a given amount of biomass burned. B and $e(X)$ are functions of the land cover classification and BE is a function of the tree cover. The species considered are CO, CO_2, NO_x, SO_2, NH_3, $PM_{2.5}$ and PM_{10}.

In this study, the burnt area is obtained from MODIS Collection 5 Burned Area Product - MCD45. The NASA Moderate Resolution Imaging Spectroradiometer (MODIS) on the Terra (morning) and Aqua (afternoon) satellites has specific features for fire monitoring and has been used to systematically generate a suite of global MODIS land products [18] including a 1 km active fire product [19] and more recently a burned area product that maps the approximate day and extent of burning at 500 m resolution [20]. The type of vegetation (or fuel) that is burned, the loading of those fuels, and the proportional consumption, controlled by fuel moisture and fire intensity, determine fire emissions. To assign fuel loadings for pixels in which fires were identified, we refers to the land cover used by BOLCHEM, that is the UMD Global Land Cover Classification (GLCC), 1 Kilometer, 1.0, [21], a classification from AVHRR satellite and free available from `ftp://ftp.glcf.umiacs.umd.edu/glcf/Global_Land_Cover/Global`. The Global Land Cover Classification characterizes the global land cover with 14 different classes at a resolution of 1 km. The core of our work has been first to establish correspondence between the GLC2000 vegetation cover classes [12, 22, 23] and the UMD GLCC, and then to estimated values of fuel load and burning efficiency at each class of vegetation. Finally, for any vegetation type, we have assigned emissions factor at the different emitted species [24-26, 9, 27].

Emissions are supposed to not be constant during the day. Several studies based on satellite and *in situ* measurements (*e.g.*, [28, 17]) have suggested that biomass burning exhibits a pronounced diurnal cycle with peak emissions during early afternoon (13–16 h UTC) and very low emissions during the night. Therefore the WRAP diurnal profile is applied.

2˙2. *Injection height.* – The injection height is related to the flaming intensity of the fire and can be estimated based on fire characteristics (such as the fire size or temperature) and atmospheric conditions. In this study, we use the approach from the WRAP method [17] in which fires are classified into size classes based on virtual acreage. The virtual acreage is calculated by multiplying the fire size by the square root of the normalized pre-burn fuel loading:

$$Acreage_{\text{virtual}} = Acreage_{\text{actual}} \cdot \sqrt{\frac{Fuel\ load}{Normalizer}}, \tag{2}$$

where $Normalizer = 13.8 \cdot 10^{-3}$ kg.

Five plume classes were defined with increasing potential plume heights to reflect the range of heat release possible in wildland fires (table I). Plume bottom heights and

TABLE I. – *Fire-related parameters as a function of fire size classes.*

Class	1	2	3	4	5
Size (virtual acreage)	0–10	10–100	100–1000	1000–5000	> 5000
BE_{size}	0.40	0.60	0.75	0.85	0.90
$Ptop_{\max}$(m)	160	2400	6400	7200	8000
$Ptop_{\min}$(m)	0	900	2200	3000	3000

percent of the plume fumigated to the first layer of the atmosphere were also developed for the five plume classes. Using expert opinion, hourly buoyant efficiency values was derived.

The hourly top and bottom of the plume will be calculated as follows:

$$Ptop_{\text{hour}} = BE_{\text{hour}} \cdot BE_{\text{size}} \cdot Ptop_{\max}, \tag{3}$$

$$Pbot_{\text{hour}} = BE_{\text{hour}} \cdot BE_{\text{size}} \cdot Pbot_{\max}. \tag{4}$$

where BE_{size} is the buoyant efficiency from the size class (see table I) and BE_{hour} is the hourly bouyant efficiency.

3. – The BOLCHEM model: description and set-up

In order to study the dispersion of gases and particulate from wildfires, emissions and injection heights from wildfires have been included in BOLCHEM. BOLCHEM [29] is an air quality model which couples online meteorology and atmospheric chemistry. It solves the primitive hydrostatic equation for meteorology (BOLAM [30]) and gas phase chemistry (SAPRC90 [31]) and aerosol dynamics (AERO3 [32]). The methodology described in the previous section is applied to build a pre-processor prebolchem_fire for wildfires emission starting from geographic position of fires and providing emissions as input for BOLCHEM. New routines for taking into account the wildfires emissions of gas and particulate and the injection height have been added in BOLCHEM. Simulations of wildfires occurred in Greece, Albania and Algeria during the period 22-30 August 2007 have been performed to study their impact on the air quality.

In order to include the above-mentioned wildfires, the model domain used in this study includes Europe and North Africa: NW (−5°, 51°); NE(30°, 51°); SW(−5°, 31°); SE(30°, 31°). The horizontal resolution is 25 km while the vertical grid has 40 sigma layers with the lowest layer approximately 40 m thick. The initial and boundary conditions for meteorology are supplied by ECMWF. The lateral boundary conditions are updated every 6 h. The weather fields are re-initialised every 24 h with the ECMWF analyses in order to avoid an excessive error growth in the meteorological simulation.

Climatological boundary conditions are used for atmospheric composition as the simulation domain is large enough to avoid the influence of external sources.

The wildfire emissions fields are added to the anthropogenic and biogenic emissions. The anthropogenic emission fields have been generated from the TNO inventory for the 2003 year and made available in the frame of GEMS project [33,34]. The TNO inventory

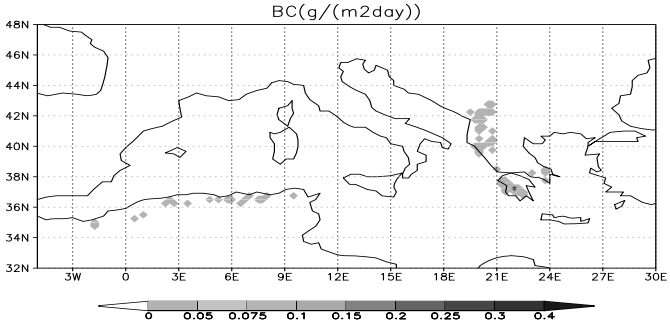

Fig. 1. – Daily emission flux of BC (g/(m^2 d)) for 26 August 2007.

provides annual data at the spatial resolution of 1/8° of longitude and 1/16° of latitude. The annual emissions amounts were split in time to hourly resolution and VOCs, NO_x, and PM_{10} were chemically speciated on the basis of daily, weekly and seasonal activity profiles derived by literature [35]. Biogenic emissions are based on an inventory providing potential emissions and generated by NKUA (National and Kapodistrian University of Athens) in the frame of GEMS project. Finally, wildfires emissions are based on the pre-processor build following the methodology described in sect. **2**. To be suitable for SAPRC90 module, NO_x and $PM_{2.5}$ are disaggregated, respectively, as follows: NO_x = 95% NO_2 + 5% NO; $PM_{2.5}$ = 10%BC + 86%OC + 4%S. The coarse mode is obtained from the difference between PM_{10} and $PM_{2.5}$. Black carbon (BC), organic carbon (OC) and sulphites (S) are then divided into accumulation (99%) and aitken (1%) modes. References about disaggregation adopted in this work are [36, 32, 37]. Two simulations have been performed. The first one includes anthropogenic, biogenic and wildfire emissions (ant-bio-fire); the second one anthropogenic and biogenic emissions (ant-bio).

4. – Results

This section discusses the model results for wildfires occurred in Greece, Albania and Algeria from 22 to 30 August 2007.

4˙1. *Emissions flux and injection height*. – The methodology described in sect. **2** was applied to calculate emissions and injection height for wildfires in Greece, Algeria and Albania. As an example, fig. 1 shows emission fluxes of BC, output of the model prebolchem_fire and input of BOLCHEM simulations, for 26 August 2007 whereas fig. 2 shows an example of diurnal cycle of BC (g/(m^2 h)) and injection heights for 26 August 2007 at 21.7°E/37.5°N longitude/latitude (Greece). Both figures display a peak emissions during early afternoon (13–16 h UTC) and very low emissions during the night.

Figure 1 shows that the flux emissions of BC, for 26 August 2007, ranges from 0.1 to more than 0.4 g/m^2 per day. Figures 2 show a peak emissions during early afternoon (13–16 h UTC) and very low emissions during the night. During the night fire emits just in the boundary layer, while during early afternoon (13–16 h UTC) fire emits totally in the troposphere, being the injection height between 2000 and 5500 meters.

To test the developed emission flux methodology, we have compared the estimated gas and particulate emissions with those estimated by the global model FINNv1 (Fire

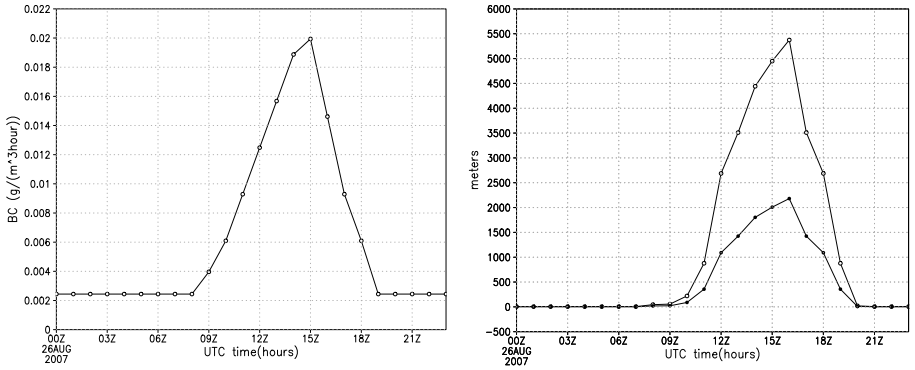

Fig. 2. – Diurnal cycle of hourly flux emission of BC (left) and of injection height (right) for 26 August 2007 at longitude = 21.7°E /37.5°N longitude/latitude (Greece).

INventory from NCAR), that provides daily estimate of gas and particulate from wildfires at 1 km^2 of resolution [11,12]. We point out that a quantitative assignment of uncertainty is difficult, due to the uncertainties associated with the land cover classifications, the fire detections, the assumed area burned, the biomass loading, the amount of fuel burned, and emission factors. At this time, we follow other efforts (*e.g.*, [12, 23]) and assign the uncertainty as a factor of two for the estimates.

Figure 3 shows daily quantity of CO, NO_2, $PM_{2.5}$ and PM_{10} emitted from wildfires estimated by prebolchemifire (circle point) and FINNv1 model (square points), with the uncertainties calculated as described above.

From fig. 3 we can infer that our model overestimates wildfires emissions, mainly for CO and NO_2. Differences are major when a peak of emissions is estimated (26 and 27 August 2007), and only the 27 estimates does not overlap. Regarding particulate ($PM_{2.5}$ and PM_{10}), for each day estimates are overlapping. The agreement is better when we

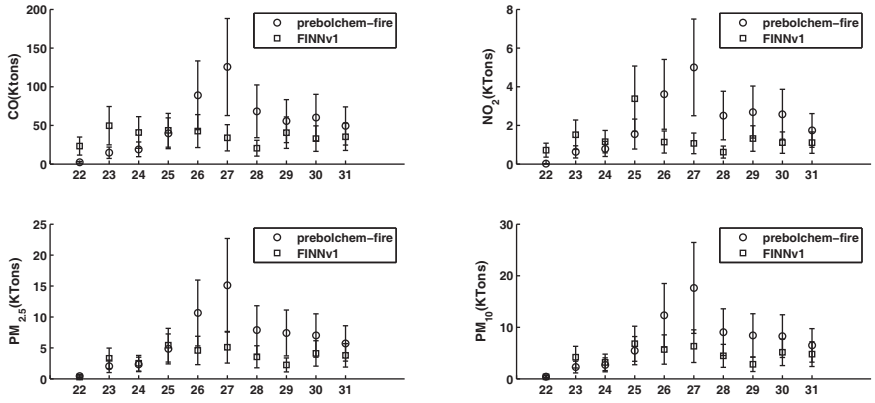

Fig. 3. – Quantity and uncertainties of CO, NO_2, $PM_{2.5}$ and PM_{10} estimated by prebolchemfire model (circles) and FINNv1 model (squares).

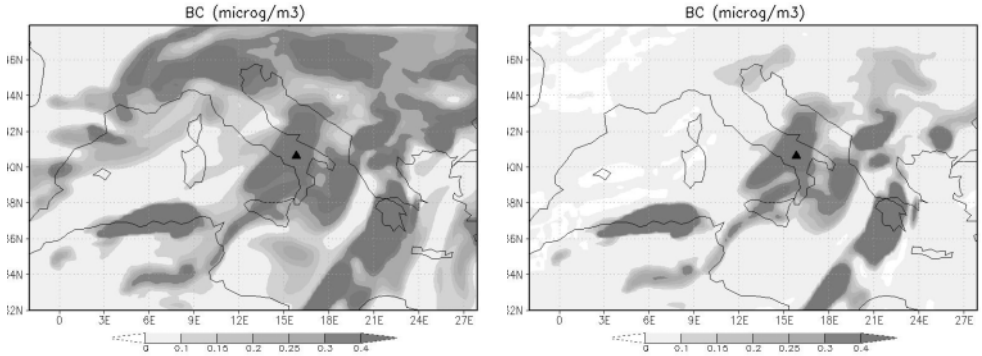

Fig. 4. – Concentration maps of BC (μg/m^3) at about 1500 meters for 30 August 2007. Left: simulation bio-ant-fire. Right: difference between simulation bio-ant-fire and bio-ant.

consider the total quantity emitted during the period case study (results not shown). Differences between the two emissions are mainly due to different data for the burned area and due to different vegetation maps, whereas the methodology is the same. In particular, we used the data set MODIS area burned whereas the author of FINNv1 used the data set MODIS Thermal Anomalies Product [7]. The landuse description that we incorporate is based on 14 classes of vegetation, the land followed the description used by the FINNv1 authors is based on 29 classes of vegetation.

4˙2. *Results of numerical simulation*. – We have compared the vertical distribution of BC concentration simulated with BOLCHEM with lidar observations at Tito Scalo, Potenza (40.63 N, 15.80 E, 760 m a.s.l.). Here, an unusual layer of aerosol has been detected by the PEARL station lidar on 30 August 2007 above 4800 meters of altitude. Figure 5b) shows the backscatter coefficient profile measured in PEARL station. The study of backscatter coefficient lead to suppose that the aerosol layer between the boundery layer and 4800 meters is containing the typical characteristic of the particulate from forest fire [38].

Regarding the meteorological situation, the BOLAM simulation (here not displayed) for 24 August 2007 highlighted that the passage of a trough over West Europe favoured the transport of air masses from North Africa to the central Mediterranean and Italy. From 25 to 28 August 2007 the low tropospheric circulation over the central Mediterranean basin was instead determined by a high-pressure ridge centred over Sardinia, favouring the transport of air masses from North Africa towards northern Italy. From 28 August 2007 a low-pressure trough affected Western Europe, again favouring air mass transport from North Africa toward northern and central Italy. The end of air mass advection from North Africa, around 31 August 2007, was related to the eastward displacement of the low-pressure system, which induced a westerly flow over northern Italy.

Results of simulations are shown in figs. 4 and 5. In particular, fig. 4 shows the concentration of BC aerosol for 30 August 2007 at 6 pm at about 1500 m for (left) the simulation bio-ant-fire and for (right) the difference between the simulation bio-ant-fire and bio-ant. The map on the right of the figure puts in evidence the contribution of wildfire emission of BC to PEARL station (triangle) and, in general, to the centre-south of Italy at 1500 metres. Figure 5a) shows the profile of BC at the PEARL station for

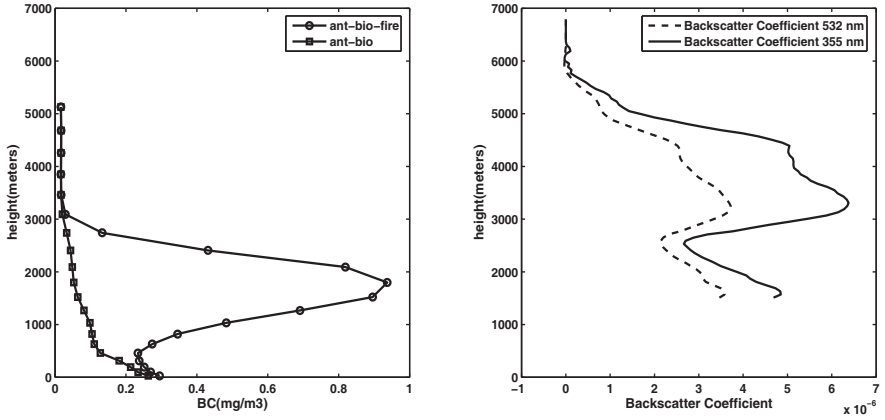

Fig. 5. – Right: BC concentration profile from BOLCHEM outputs; left: backscatter profiles measured in PEARL station. Profiles are for 30 August 2007 at 18 hour.

the simulation bio-ant-fire (circle) and ant-bio (square). From this figure we can infer that wildfires emissions of BC contribute to the air quality on Potenza from the surface to about 3000 m. The profile obtained from lidar observations is not well reproduced by BOLCHEM simulation at high altitudes and, at lower heights, the simulations show a higher contribution of BC from wildfire emissions than lidar measurements. The difference is probably due to an inaccurate representation of the vertical transport and the convective motions in BOLCHEM. Also a not very realistic representation of wildfires emission and injection height can explain the difference between profiles. Further work will be carried out to investigate the sensitivity of BOLCHEM simulation results to emissions flux and injection heights, and to compare the output model with different measurement stations data (*e.g.* Monte Cimone [39], Athens [40]) The inclusion of the AOD (Aerosol Optical Depth) module (work in progress) in BOLCHEM will lead to a comparison of numerical results of AOD with AOD maps from Satellite data (*e.g.*, CALIPSO—Cloud Aerosol Lidar and Infrared Pathfinder Satellite Observation).

REFERENCES

[1] Crutzen P. J. and Andreae M. O., *Science*, **250** (1990) 1169.
[2] Val Martin M., Honrath R., Owen R. C., Pfister G., Fialho P. and Barata F., *J. Geophys. Res.*, **111** (2006) D23S60.
[3] Seiler W. and Crutzen P. J., *Clim. Change*, **2** (1980) 207.
[4] Hao W. M. and Liu M., *Global Biogeochem. Cycles*, **8** (1994) 495.
[5] Schultz W. M., *Atmos. Chem. Phys.*, **2** (2002) 387.
[6] Gregoire J. M., Tansey K. and Silva M. N., *Int. J. Remote Sens.*, **24** (2003) 1369.
[7] Giglio L., Csiszar I. and Justice O., *J. Geophys. Res.*, **111** (2006) doi:10.1029/2005JG000142.
[8] Hoelzemann J., Plummer S., Fierens F., Hoelzemann H. H. and Arino O., *Int. J. Geophys. Res.*, **109** (2004) doi:10.1029/2003JD003622.
[9] Hoelzemann J., Schultz M., Brasseur G., Granier C. and Simon M., *Int. J. Geophys. Res.*, **109** (2004) doi:10.1029/2003JD003666.

[10] Ito A. and Penner J. E., *Int. J. Geophys. Res.*, **109** (2004) doi:10.1029/2003JD004423.
[11] Wiedinmyer C., AKagi S. K., Yokelson R. J., Emmons L. K., Al-Saadi J. A., Orlando J. J. and Soja A. J., *Geosci. Model Dev. Discuss.*, **3** (2010) 2439.
[12] Wiedinmyer C., Quayle B., Geron B., Belote A., Mckenzie D., Zhang X. Y., ONeill S. and Winne K. K., *Atmos. Environ*, **40** (2006) 3419.
[13] Wang J., Christopher S. A, Nair U. S., Reid J. S., Prins E. M., Szykman J. and Hand J. L., *J. Geophys. Res.*, **111** (2006) doi:10.1029/2005JD006416.
[14] Damoah R., Spichtinger N., Forster C., James P., Mattis I., Wandinger U., Beirle S., Wagner T. and Stohl A., *Atmos. Chem. Phys.*, **4** (2004) 1311.
[15] Colarco P. R., Schoeberl M. R., Doddridge B. G., Marufu L. T., Torres O. and Welton E. J., *J. Geophys. Res.*, **109** (2004) doi:10.1029/2003JD004248.
[16] Hodzic A., Madronich S., Bohn B., Massie S., Menut L. and Wiedinmyer C., *Atmos. Chem. Phys.*, **7** (2007) 4043.
[17] *WRAP, Western Regional Air Partnership 2002 Fire emission inventory for the WRAP region phase II. Prepared by Air Sciences*, Inc. Project No. 178 (2005) July 22.
[18] Justice C. and Roselle S. J., *J. Geophys. Res.*, **108(D6)** (2003) doi:10.1029/2001JD001409.
[19] Giglio L., Descloitres J., Justice C. and Kaufman Y. J., *Remote Sensing Environ.*, **87** (2003) 273.
[20] Roy D. P., Jin Y., Lewis P. E. and Justice C. O., *Remote Sensing Environ.*, **97** (2005) 137.
[21] Hansen M. C., DeFries R. S., Townshend J. R. G. and Sohlberg R., *Int. J. Remote Sensing*, **21** (2000) 1331.
[22] Cinnirella S., Pirrone N., Allegrini A. and Guglietta D., *Environ. Fluid Mech.*, **8** (2008) 129.
[23] Mieville A., Granier C., Liousse C., Guillaume B., Mouillot F., Lamarque J. F., Gregoire J. M. and Petron G., *Atmos. Environ.*, **44** (2010) 1469.
[24] *EPAAP-42 document (1995) EPA, Compilation of Air Pollutant Emission Factors*, AP42, fifth ed., Vol. **1**: *Stationary Point and Area* (1995).
[25] Battye W. and Battye R., *Development of emissions inventory methods for wildland fire.*, *Final report to the U.S.EPA OAQPS*, EPA Contract No. 68D98046 (1999).
[26] Andreae M. O. and Merlet P., *Global Biogeochemical Cycles*, **15** (2001) 995.
[27] Liu Y., *Atmospheric Environment*, **38** (2004) 3489.
[28] Eck T. M., Holben B. N., Reid J. S., Oǵeill N. T., Schafer J. S., Dubovik O., Smirnov A. and Yamasoe M., *Geophys. Res. Lett.*, **30** (2003) doi:10.10292003GL018697.
[29] Mircea M., D'Isidoro M., Maurizi A., Vitali L., Monforti F., Zanini G. and Tampieri F., *Atmospheric Environment*, **42** (2008) 1169.
[30] Buzzi A., Fantini M., Malaguzzi P. and Nerozzi P., *Meteor. Atmos. Phys.*, **53** (1994) 137.
[31] Carter W. P. L., *Atm. Environ.*, **24A** (1990) 481.
[32] Binkowski F. S. and Roselle S. J., *J. Geophys. Res.*, **108(D6)** (2003) doi:10.1029/2001JD001409.
[33] Visschedijk A. and van der Gon H. D., *Gridded European Anthropogenic Emission Data for NOx, SO2, NMVOC, NH3, CO, PM10, PM2.5 and CH4 for the Year 2000 Technical Report TNO B&O-A Rapport 2005/106*, 2nd version, TNO, Apeldoorn (2005).
[34] Visschedijk A., Zandveld P. and van der Gon H. D., *A High Resolution Gridded European Emission Database for the EU Integrated Project GEMS*, *Technical Report TNOreport 2007AR0233B*, TNO, Apeldoorn (2007).
[35] Monforti F. and Pederzoli A., *Environ. Modelling Software*, **20** (2005) 505.
[36] EPA/600/R-99/030 science algorithms of the epamodels-3 community multiscale air quality (CMAQ) modeling system (1999).
[37] *EMEP Report 1/2003, Part 1.*, 2003.
[38] Monti F., *Atmospheric aerosol transport analysis:integration between theoretical models and experimental measurements.*, Phd Thesis, Universitá degli Studi della Basilicata (Pz) (2009).

[39] Cristofanelli P., Marinoni A., Arduini J., Bonafé U., Calzolari F., Colombo T., Decesari S., Duchi R., Facchini M.C., Fierli F., Finessi E., Maione M., Chiari M., Calzolai G., Messina P., Orlandi E., Roccato F. and Bonasoni P., *Atmos. Chem. Phys. Discuss.*, **9** (2009) 7825.
[40] Liu Y., Kahn R. A., Chaloulakou A. and Koutrakis P., *Atm. Environ.*, **43** (2009) 3310.